Available online at www.sciencedirect.com
SCIENCE DIRECT®
International Journal of Solids and Structures 42 (2005) 2803–2822
INTERNATIONAL JOURNAL OF SOLIDS and STRUCTURES
www.elsevier.com/locate/ijsolstr

Stress and electric displacement analyses in piezoelectric media with an elliptic hole and a small crack

Zhi-Dong Zhou, She-Xu Zhao, Zhen-Bang Kuang *

Department of Engineering Mechanics, Shanghai Jiaotong University, Shanghai 200240, PR China

Received 5 April 2004; received in revised form 24 September 2004
Available online 26 November 2004

Abstract

In this paper, the interactions between an elliptic hole and an arbitrary distributed small crack in plane piezoelectric medium, which are often happened in engineering problems, are discussed. The Green's functions in a piezoelectric plate with an elliptic hole for a generalized line dislocation and a generalized line force are presented. The small crack is represented by unknown continuous distributed dislocations. By considering traction free conditions on the surface of the small crack, the problem is then reduced to a group of singular integral equations which are solved by using a special numerical technique. Accuracy of the present method is confirmed by comparing the numerical results with those in literatures for PZT-4 when the elliptic hole is degenerated into a crack. The generalized stress intensity factors of cracks and the generalized stress on the edge of the elliptic hole are shown graphically. It is shown that the small crack may have shielding or amplifying effects on the main elliptic hole or crack, which depends on the location and orientation of the small crack. The hole near a crack can significantly reduce the stress intensity factor of the crack. The direction of the electric field is important to shielding effect.

Keywords: Fracture; Piezoelectric; Small crack; Singular integral equation; Green's function

1. Introduction

Piezoelectric ceramics are widely used as smart materials owing to their strong coupling between electric and mechanical fields. Because piezoelectric ceramics are very brittle and susceptible to fracture, the linear fracture behaviors of these materials under combined electro-mechanical loads have drawn increasing attention in many researches (Sosa, 1991; Pak, 1992; Suo et al., 1992; Park and Sun, 1995; Sosa and

* Corresponding author. Tel.: +86 2154743067; fax: +86 2154743044.
E-mail address: zbkuang@mail.sjtu.edu.cn (Z.-B. Kuang).

0020-7683/$ - see front matter © 2004 Elsevier Ltd. All rights reserved.
doi:10.1016/j.ijsolstr.2004.09.038

Khutoryansky, 1996; Gao and Fan, 1999; Kuang and Ma, 2002). The analytical solutions of the problems are often restricted to some special cases, such as an infinite body with single crack under uniform loading at infinity. The problems in engineering always possess some defects and the closed solution cannot be obtained easily. So the Green's functions and numerical methods are necessary for these complex problems. Lu and Williams (1998) and Gao and Fan (1998) obtained the Green's functions in an infinite 2-D piezoelectric material with an elliptic hole for a generalized line force. Huang and Kuang (2001) obtained Green's functions in an infinite piezoelectric medium containing an elliptic piezoelectric inhomogeneity for a generalized line dislocation and a generalized line force. Wu et al. (1978) reported that small cracks significantly contribute to the overall failure mechanism in brittle materials. Han and Chen (1999) studied the multiple parallel cracks interaction in a transversely isotropic piezoelectric material. Zeng and Rajapakse (2000) investigated theoretically the interaction between a semi-infinite main crack and an arbitrary distributed small crack in a piezoelectric plate. The pseudo-tractions method is usually used to solve these interaction problems. Hwu et al. (1995) researched the interactions between inclusions and various distributions of cracks for the anisotropic elastic materials. To our knowledge, the study on the interactions between an elliptic hole and an arbitrarily distributed small crack in plane piezoelectric medium has not been reported in literatures. In manufacturing and domain switching processes, voids and small cracks in piezoelectric ceramics may be induced (Subbarao et al., 1993). Researching the interaction between an elliptic hole and a small crack is important to the fracture of a structure.

In this paper, the Green's functions for a generalized line dislocation and a generalized line force in plane piezoelectric medium with an elliptic hole filled with or without air are presented and applied to study the interactions between an elliptic hole and an arbitrary distributed small crack. It is assumed that the air filled in the elliptic hole is a dielectric, but air cannot sustain mechanical load. This problem has simpler solution as discussed here. The small crack is treated as continuous distributed generalized line dislocations. The traction free and electrically impermeable conditions along the small crack surface will give a group of singular integral equations of the Cauchy type. The special numerical technique (Erdogan and Gupta, 1972; Hills, 1995) is introduced to solve the singular integral equations with the single-valued conditions of the displacements and electric potential. Then the generalized stress field on the edge of the elliptic hole and the generalized stress intensity factors near the tips of cracks are obtained. Numerical results show that the distributions of stress and electric displacement on the edge of the elliptic hole depend on the geometric configuration, the loading, the location and orientation of the small crack. An elliptic hole near the crack can strongly reduce the stress intensity factor of the crack and the direction of the electric field significantly influences the shielding effect. In the case that the elliptic hole is degenerated into a crack, the small crack has shielding or amplifying effect on the stress intensity factors of the main crack, which depends on the location and direction of the small crack.

2. Basic equations and general solution

In a fixed rectangular coordinate system $x_i\,(i=1,2,3)$, all of the field variables depend on x_1, x_2 only for a generalized plane piezoelectric problem. Following Suo et al. (1992), Chung and Ting (1996) and Kuang and Ma (2002), the general solution in this case can be given by the linear combination of four complex analytical functions

$$\mathbf{u}=2\,\mathrm{Re}[\mathbf{A}\mathbf{f}(z)],\quad \boldsymbol{\phi}=2\,\mathrm{Re}[\mathbf{B}\mathbf{f}(z)],$$

$$\mathbf{u}=[u_1,u_2,u_3,\varphi]^{\mathrm{T}},\quad \boldsymbol{\phi}=[\phi_1,\phi_2,\phi_3,\phi_4]^{\mathrm{T}},$$

$$\mathbf{f}(z)=[f_1(z_1),f_2(z_2),f_3(z_3),f_4(z_4)]^{\mathrm{T}},\quad z_k=x_1+p_kx_2,\ \ k=1,2,3,4, \tag{1}$$

where Re stands for the real part of a complex function; u_i, φ and ϕ_i are the displacement components, electric potential and generalized stress functions, respectively; $\mathbf{A}$ and $\mathbf{B}$ are 4×4 complex matrices related to the material constants, expressed as

$$\mathbf{A}=[\mathbf{a}_1,\mathbf{a}_2,\mathbf{a}_3,\mathbf{a}_4],\quad \mathbf{B}=[\mathbf{b}_1,\mathbf{b}_2,\mathbf{b}_3,\mathbf{b}_4]. \tag{2}$$

The eigenvalues p_k and eigenvectors $\mathbf{a}_k$ are determined by the following equations

$$[\mathbf{Q}+(\mathbf{R}+\mathbf{R}^{\mathrm{T}})p+\mathbf{T}p^2]\mathbf{a}=0, \tag{3}$$

in which

$$\mathbf{Q}=\begin{bmatrix}\mathbf{Q}^{\mathrm{E}} & \mathbf{e}_{11}\\ \mathbf{e}_{11}^{\mathrm{T}} & -\kappa_{11}\end{bmatrix},\quad \mathbf{R}=\begin{bmatrix}\mathbf{R}^{\mathrm{E}} & \mathbf{e}_{21}\\ \mathbf{e}_{21}^{\mathrm{T}} & -\kappa_{12}\end{bmatrix},\quad \mathbf{T}=\begin{bmatrix}\mathbf{T}^{\mathrm{E}} & \mathbf{e}_{22}\\ \mathbf{e}_{22}^{\mathrm{T}} & -\kappa_{22}\end{bmatrix},$$

$$Q_{ik}^{\mathrm{E}}=c_{i1k1},\quad R_{ik}^{\mathrm{E}}=c_{i1k2},\quad T_{ik}^{\mathrm{E}}=c_{i2k2},\quad (\mathbf{e}_{ij})_s=e_{ijs}, \tag{4}$$

where c_{ijkl} is the elastic stiffness under constant electric field, e_{ijs} is the piezoelectric constant and κ_{ij} is the permittivity under constant strain field. $\mathbf{b}_k$ can be obtained as

$$\mathbf{b}_k=(\mathbf{R}^{\mathrm{T}}+p_k\mathbf{T})\mathbf{a}_k=-\frac{1}{p_k}(\mathbf{Q}+p_k\mathbf{R})\mathbf{a}_k. \tag{5}$$

The generalized stress can be represented as

$$\begin{aligned}\boldsymbol{\sigma}_1&=[\sigma_{11},\sigma_{12},\sigma_{13},D_1]^{\mathrm{T}}=-[\phi_{1,2},\phi_{2,2},\phi_{3,2},\phi_{4,2}]^{\mathrm{T}},\\ \boldsymbol{\sigma}_2&=[\sigma_{21},\sigma_{22},\sigma_{23},D_2]^{\mathrm{T}}=[\phi_{1,1},\phi_{2,1},\phi_{3,1},\phi_{4,1}]^{\mathrm{T}}.\end{aligned} \tag{6}$$

After the normalization for the eigenvectors $\mathbf{A}$ and $\mathbf{B}$, the following relation can be obtained

$$\begin{bmatrix}\mathbf{B}^{\mathrm{T}} & \mathbf{A}^{\mathrm{T}}\\ \overline{\mathbf{B}}^{\mathrm{T}} & \overline{\mathbf{A}}^{\mathrm{T}}\end{bmatrix}\begin{bmatrix}\mathbf{A} & \overline{\mathbf{A}}\\ \mathbf{B} & \overline{\mathbf{B}}\end{bmatrix}=\begin{bmatrix}\mathbf{I} & 0\\ 0 & \mathbf{I}\end{bmatrix},\quad \begin{bmatrix}\mathbf{A} & \overline{\mathbf{A}}\\ \mathbf{B} & \overline{\mathbf{B}}\end{bmatrix}\begin{bmatrix}\mathbf{B}^{\mathrm{T}} & \mathbf{A}^{\mathrm{T}}\\ \overline{\mathbf{B}}^{\mathrm{T}} & \overline{\mathbf{A}}^{\mathrm{T}}\end{bmatrix}=\begin{bmatrix}\mathbf{I} & 0\\ 0 & \mathbf{I}\end{bmatrix}, \tag{7}$$

where the overbar denotes the conjugate of a complex function. The piezoelectric Barnett–Lothe tensors can be written as

$$\mathbf{S}=\mathrm{i}(2\mathbf{A}\mathbf{B}^{\mathrm{T}}-\mathbf{I}),\quad \mathbf{H}=\mathrm{i}2\mathbf{A}\mathbf{A}^{\mathrm{T}},\quad \mathbf{L}=-\mathrm{i}2\mathbf{B}\mathbf{B}^{\mathrm{T}}, \tag{8}$$

where $\mathbf{S}$, $\mathbf{H}$ and $\mathbf{L}$ are real, $\mathbf{H}$ and $\mathbf{L}$ are symmetric, $\mathbf{SH}$ and $\mathbf{LS}$ are antisymmetric.

3. Green's function of an infinite piezoelectric plate with an elliptic hole

Consider an infinite plane piezoelectric medium containing an elliptic hole filled with air. The geometric equation of an ellipse can be expressed as

$$\begin{aligned}&x_1=a\cos\theta,\quad x_2=b\sin\theta,\quad \rho(\theta)=\sqrt{a^2\sin^2\theta+b^2\cos^2\theta},\\ &\underline{\mathbf{n}}=\left[\frac{\mathrm{d}x_1}{\mathrm{d}s},\frac{\mathrm{d}x_2}{\mathrm{d}s},0\right]^{\mathrm{T}},\quad \underline{\mathbf{m}}=\left[-\frac{\mathrm{d}x_2}{\mathrm{d}s},\frac{\mathrm{d}x_1}{\mathrm{d}s},0\right]^{\mathrm{T}},\quad \mathrm{d}s=\rho(\theta)\,\mathrm{d}\theta,\end{aligned} \tag{9}$$

where $2a$ and $2b$ are the length of the major and minor axes of the ellipse, respectively, θ is a real parameter, $\underline{\mathbf{n}}$ and $\underline{\mathbf{m}}$ are the unit vectors tangential and normal to the elliptic boundary respectively, and s is an arc-length on the ellipse, as shown in Fig. 1. It is noted here that $\underline{\mathbf{m}}$ is pointed into the inner of the ellipse as adopted by Chung and Ting (1996).

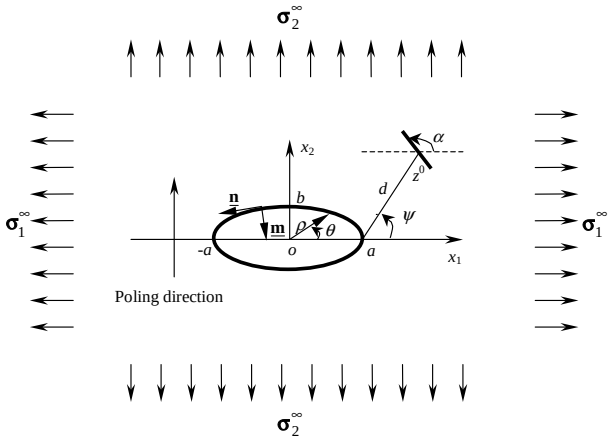

Fig. 1. An elliptic hole and a small crack in an infinite piezoelectric medium.

The mapping function

$$z_k(\varsigma_k) = c_k\varsigma_k + d_k\varsigma_k^{-1}, \quad c_k = (a - \mathrm{i}p_k b)/2, \quad d_k = (a + \mathrm{i}p_k b)/2 \tag{10}$$

will transform an ellipse in the z_k-plane into a unit circle in the ς_k-plane. The inverse mapping function is

$$\varsigma_k = \frac{z_k + \sqrt{z_k^2 - 4c_k d_k}}{2c_k}. \tag{11}$$

Along the unit circle boundary Γ, there is

$$\varsigma_k|_{\Gamma} = \sigma = \mathrm{e}^{\mathrm{i}\theta} = \cos\theta + \mathrm{i}\sin\theta. \tag{12}$$

Let the generalized line dislocation $\mathbf{b}^*$ and the generalized line force $\mathbf{f}^*$ be applied at a point $z_0(x_{10}, x_{20})$ outside the ellipse, where $\mathbf{b}^* = \{\mathbf{b}, b_4\} = \{b_1, b_2, b_3, b_4\}$, $\mathbf{b}$ represents Burgers vector and b_4 is an electric dipole layer along the slip plane, and $\mathbf{f}^* = \{\mathbf{f}, f_4\} = \{f_1, f_2, f_3, f_4\}$, $\mathbf{f}$ represents a line distributed force vector and f_4 represents a line charge. Owing to the linear property, the principle of superposition can be used and this problem can be divided into following two problems: (1) The generalized line dislocation $\mathbf{b}^*$ and the generalized line force $\mathbf{f}^*$ at the point $z_0(x_{10}, x_{20})$ in a homogeneous infinite piezoelectric medium. (2) The boundary of the elliptic hole are subjected to the loadings which makes the mechanical traction free and normal electric displacement and electric potential continuous on it with the infinite outer medium.

3.1. Infinite homogeneous piezoelectric medium subjected to $\boldsymbol{b}^*$ and $\boldsymbol{f}^*$ at a point

For the case that the generalized line dislocation $\mathbf{b}^*$ and the generalized line force $\mathbf{f}^*$ are applied at a point $z_0(x_{10}, x_{20})$ in a homogeneous infinite piezoelectric medium (problem (1)), the generalized stress function and generalized displacement can be written as

$$\mathbf{u}^{\mathrm{I}} = 2\,\mathrm{Re}[\mathbf{A}\mathbf{f}^{\mathrm{I}}(z)], \quad \boldsymbol{\phi}^{\mathrm{I}} = 2\,\mathrm{Re}[\mathbf{B}\mathbf{f}^{\mathrm{I}}(z)], \tag{13a}$$

or

$$u_j^{\mathrm{I}} = 2\,\mathrm{Re}[a_{jk} f_k^{\mathrm{I}}(z_k)], \quad \phi_j^{\mathrm{I}} = 2\,\mathrm{Re}[b_{jk} f_k^{\mathrm{I}}(z_k)], \tag{13b}$$

$$f_k^{\mathrm{I}}(z_k) = q_k \ln(z_k - z_{k0}), \quad z_{k0} = x_{10} + p_k x_{20}. \tag{13c}$$

The equilibrium conditions of the force and the single-valued conditions of the generalized displacement are

$$\oint_c \mathrm{d}\boldsymbol{\phi}^{\mathrm{I}} = \mathbf{f}^*, \quad \oint_c \mathrm{d}\mathbf{u}^{\mathrm{I}} = \mathbf{b}^*, \tag{14a}$$

where c presents an arbitrary closed curve around the point z_0. Combining Eq. (13) with Eq. (14a), it is found

$$4\pi \mathrm{Re}[\mathrm{i}\mathbf{B}\mathbf{q}] = \mathbf{f}^*, \quad 4\pi \mathrm{Re}[\mathrm{i}\mathbf{A}\mathbf{q}] = \mathbf{b}^*. \tag{14b}$$

With the aid of Eq. $(7)_1$, the following relation can be obtained

$$\mathbf{q} = \frac{1}{2\pi\mathrm{i}}\mathbf{A}^{\mathrm{T}}\mathbf{f}^* + \frac{1}{2\pi\mathrm{i}}\mathbf{B}^{\mathrm{T}}\mathbf{b}^*. \tag{15}$$

According to the principle of superposition cited above, it is needed for problem (2) to obtain the surface traction along the elliptic boundary. In doing so, the generalized stress function along the elliptic boundary is firstly solved as follows.

By using Eqs. (12), (13) and (15) and the relation

$$\ln[z_k(\varsigma_k) - z_{k0}(\varsigma_{k0})] = \ln(\varsigma_k - \varsigma_{k0}) + \ln\left[c_k\left(1 - \frac{d_k/c_k}{\varsigma_k\varsigma_{k0}}\right)\right], \tag{16}$$

the generalized stress function due to the presence of the generalized line dislocation and the generalized force at z_0 can be obtained as

$$\boldsymbol{\phi}^{\mathrm{I}} = \frac{1}{\pi}\mathrm{Im}\left\{\mathbf{B}\left\langle \ln(\varsigma_k - \varsigma_{k0}) + \ln\left[c_k\left(1 - \frac{d_k/c_k}{\varsigma_k\varsigma_{k0}}\right)\right]\right\rangle(\mathbf{A}^{\mathrm{T}}\mathbf{f}^* + \mathbf{B}^{\mathrm{T}}\mathbf{b}^*)\right\}. \tag{17}$$

Along the unit circle boundary, it follows

$$\boldsymbol{\phi}^{\mathrm{I}}_{\Gamma} = \frac{1}{\pi}\mathrm{Im}\left\{\mathbf{B}\left\langle \ln(\sigma - \varsigma_{k0}) + \ln\left[c_k\left(1 - \frac{d_k/c_k}{\sigma\varsigma_{k0}}\right)\right]\right\rangle(\mathbf{A}^{\mathrm{T}}\mathbf{f}^* + \mathbf{B}^{\mathrm{T}}\mathbf{b}^*)\right\}, \tag{18}$$

in which $\langle\bullet\rangle$represents a diagonal matrix, Im stands for the imaginary part of a complex function, and

$$\begin{aligned}
&\ln(\sigma - \varsigma_{k0}) = \ln(-\varsigma_{k0}) - \sum_{n=1}^{\infty}\frac{1}{n}\left(\frac{\sigma}{\varsigma_{k0}}\right)^n = \ln(-\varsigma_{k0}) - \sum_{n=1}^{\infty}\frac{1}{n}\left(\frac{1}{\varsigma_{k0}}\right)^n[\cos(n\theta) + \mathrm{i}\sin(n\theta)],\\
&\ln\left[c_k\left(1 - \frac{d_k/c_k}{\sigma\varsigma_{k0}}\right)\right] = \ln c_k - \sum_{n=1}^{\infty}\frac{1}{n}\left(\frac{d_k/c_k}{\sigma\varsigma_{k0}}\right)^n = \ln c_k - \sum_{n=1}^{\infty}\frac{1}{n}\left(\frac{d_k/c_k}{\varsigma_{k0}}\right)^n[\cos(n\theta) - \mathrm{i}\sin(n\theta)].
\end{aligned} \tag{19}$$

Applying Eq. (6), the generalized surface traction vector $\mathbf{t}_{\underline{m}}$ at a point on the elliptic boundary in this case can be obtained as

$$\begin{aligned}
\mathbf{t}_{\underline{m}} &= (\boldsymbol{\phi}^{\mathrm{I}}_{\Gamma})_{,s}\\
&= \frac{1}{\pi\rho(\theta)}\mathrm{Im}\left\{\mathbf{B}\left\langle \sum_{n=1}^{\infty}\left\{\left[\left(\frac{1}{\varsigma_{k0}}\right)^n + \left(\frac{d_k/c_k}{\varsigma_{k0}}\right)^n\right]\sin(n\theta)\right.\right.\\
&\quad \left.\left. + \mathrm{i}\left[\left(\frac{d_k/c_k}{\varsigma_{k0}}\right)^n - \left(\frac{1}{\varsigma_{k0}}\right)^n\right]\cos(n\theta)\right\}\right\rangle(\mathbf{A}^{\mathrm{T}}\mathbf{f}^* + \mathbf{B}^{\mathrm{T}}\mathbf{b}^*)\Bigg\}.
\end{aligned} \tag{20}$$

3.2. The general solution of an infinite piezoelectric medium with an elliptic hole

For problem (2), the generalized displacement and stress function vanishing at infinity in the piezoelectric medium can be expressed as (Chung and Ting, 1996)

$$\begin{aligned}
\mathbf{f}^{\mathrm{II}}(z) &= \langle \varsigma_k^{-n} \rangle (\mathbf{A}^{\mathrm{T}}\mathbf{g}_n + \mathbf{B}^{\mathrm{T}}\mathbf{h}_n), \\
\mathbf{u}^{\mathrm{II}} &= 2\sum_{n=1}^{\infty} \mathrm{Re}[\mathbf{A}\langle \varsigma_k^{-n} \rangle \mathbf{A}^{\mathrm{T}}]\mathbf{g}_n + 2\sum_{n=1}^{\infty} \mathrm{Re}[\mathbf{A}\langle \varsigma_k^{-n} \rangle \mathbf{B}^{\mathrm{T}}]\mathbf{h}_n, \\
\boldsymbol{\phi}^{\mathrm{II}} &= 2\sum_{n=1}^{\infty} \mathrm{Re}[\mathbf{B}\langle \varsigma_k^{-n} \rangle \mathbf{A}^{\mathrm{T}}]\mathbf{g}_n + 2\sum_{n=1}^{\infty} \mathrm{Re}[\mathbf{B}\langle \varsigma_k^{-n} \rangle \mathbf{B}^{\mathrm{T}}]\mathbf{h}_n,
\end{aligned} \tag{21}$$

where $\mathbf{g}_n$,$\mathbf{h}_n$ are real constant vectors, which will be determined later by the exact boundary conditions. Substituting Eq. (12) into Eq. (21), the generalized displacement, generalized stress function and the generalized surface traction $\hat{\mathbf{t}}_{\underline{m}}$ along the elliptic boundary can be expressed as

$$\begin{aligned}
\mathbf{u}_{\Gamma}^{\mathrm{II}} &= \sum_{n=1}^{\infty} [\cos(n\theta)\mathbf{h}_n - \sin(n\theta)\hat{\mathbf{h}}_n], \\
\boldsymbol{\phi}_{\Gamma}^{\mathrm{II}} &= \sum_{n=1}^{\infty} [\cos(n\theta)\mathbf{g}_n - \sin(n\theta)\hat{\mathbf{g}}_n], \\
\hat{\mathbf{t}}_{\underline{m}} &= (\boldsymbol{\phi}_{\Gamma}^{\mathrm{II}})_{,s} = -\frac{1}{\rho(\theta)} \sum_{n=1}^{\infty} \{n[\sin(n\theta)\mathbf{g}_n + \cos(n\theta)\hat{\mathbf{g}}_n]\},
\end{aligned} \tag{22}$$

in which

$$\hat{\mathbf{h}}_n = \mathbf{S}\mathbf{h}_n + \mathbf{H}\mathbf{g}_n, \quad \hat{\mathbf{g}}_n = \mathbf{S}^{\mathrm{T}}\mathbf{g}_n - \mathbf{L}\mathbf{h}_n, \quad n = 1, 2, \ldots \tag{23}$$

3.3. The electric field within the elliptic hole

On the other hand, the scalar electric potential φ_0 inside the hole without free charge can be expressed as (Gao and Fan, 1998; Zhou et al., 2004; Kuang and Ma, 2002)

$$\varphi_0(z) = 2\,\mathrm{Re}\, f_0(z), \quad -(E_1 - \mathrm{i}E_2) = -\overline{E} = \frac{2\,\mathrm{d}f_0(z)}{\mathrm{d}z}, \tag{24}$$

in which E is the electric field $f_0(z)$ is an analytical function inside the hole. If in the local coordinate system at a point on the elliptic boundary is selected such that $\underline{\mathbf{n}}$ is coincided with x_1 and $\underline{\mathbf{m}}$ is coincided with x_2, then it is easy known that the normal electric displacement component on the boundary of the hole is

$$D_{\underline{m}}^{*} = -\frac{2\varepsilon_0\,\mathrm{Im}[\mathrm{d}f_0(z)]}{\mathrm{d}s}, \quad \mathrm{d}s = \rho(\theta)\,\mathrm{d}\theta, \tag{25}$$

where ε_0 is the permittivity of air.

Because the air is isotropic, the mapping function

$$z(\varsigma_0) = c_0\varsigma_0 + d_0\varsigma_0^{-1}, \quad c_0 = (a+b)/2, \quad d_0 = (a-b)/2, \tag{26}$$

transforms the elliptic boundary into a unit circle boundary and transforms the real axis between $-\sqrt{a^2-b^2}$ and $\sqrt{a^2-b^2}$ into the circle ($\rho_0 = \sqrt{(a-b)/(a+b)} < 1$), respectively. Namely, the inside of an elliptic hole is transformed into the inside of an annular ring between $|\varsigma_0| = 1$ and $\rho_0 < 1$. Therefore, in the annular ring, $f_0(z)$ can be expressed by Laurent's expansion as

$$f_0(\varsigma_0) = \sum_{n=-\infty}^{\infty} a_n^0 \varsigma_0^n, \tag{27}$$

where a_n^0 is a complex constant. Because $f_0(z)$ is analytic inside the elliptic hole in the physical plane, the following condition on the circle with radius ρ_0 in the mapping plane must be satisfied (Sosa and Khutoryansky, 1996; Kuang and Ma, 2002)

$$f_0(\rho_0 e^{i\theta}) = f_0(\rho_0 e^{-i\theta}). \tag{28}$$

Following Eq. (28), $f_0(z)$ can be expressed as

$$f_0(\varsigma_0) = \sum_{n=1}^{\infty} a_n^0 (\varsigma_0^n + (d_0/c_0)^n \varsigma_0^{-n}). \tag{29}$$

Substituting Eqs. (12) and (29) into Eq. (25), we have

$$D^*_{\underline{m}\Gamma} = \frac{-2\varepsilon_0}{\rho_0} \sum_{n=1}^{\infty} \left\{ \left[-n\left(1 + \left(\frac{d_0}{c_0}\right)^n\right) \mathrm{Im}\, a_n^0 \right] \sin(n\theta) + \left[n\left(1 - \left(\frac{d_0}{c_0}\right)^n\right) \mathrm{Re}\, a_n^0 \right] \cos(n\theta) \right\}. \tag{30}$$

3.4. Green's function of the problem

To ensure the traction-free and electric displacement continuous conditions on the interface (boundary) of the elliptic hole and its outer infinite piezoelectric plate for the original problem, the generalized surface traction $\hat{\mathbf{t}}_{\underline{m}}$ must be applied to the elliptic boundary in problem (2), where

$$\hat{\mathbf{t}}_{\underline{m}} = -\mathbf{t}_{\underline{m}} + D^*_{\underline{m}\Gamma}\mathbf{i}_4, \quad \mathbf{i}_4 = [0,0,0,1]^{\mathrm{T}}. \tag{31}$$

Substituting Eqs. (20), $(22)_3$ and (30) into Eq. (31), the following relations can be obtained

$$\mathbf{g}_n = \mathbf{g}_n^{(1)} + \mathbf{g}_n^{(2)}, \quad \hat{\mathbf{g}}_n = \hat{\mathbf{g}}_n^{(1)} + \hat{\mathbf{g}}_n^{(2)},$$

$$\begin{cases} \mathbf{g}_n^{(1)} = \frac{1}{n\pi} \mathrm{Im}\left[\mathbf{B} \left\langle \left(\frac{1}{\varsigma_{k0}}\right)^n + \left(\frac{d_k/c_k}{\varsigma_{k0}}\right)^n \right\rangle (\mathbf{A}^{\mathrm{T}}\mathbf{f}^* + \mathbf{B}^{\mathrm{T}}\mathbf{b}^*) \right], \\ \hat{\mathbf{g}}_n^{(1)} = \frac{1}{n\pi} \mathrm{Re}\left[\mathbf{B} \left\langle \left(\frac{d_k/c_k}{\varsigma_{k0}}\right)^n - \left(\frac{1}{\varsigma_{k0}}\right)^n \right\rangle (\mathbf{A}^{\mathrm{T}}\mathbf{f}^* + \mathbf{B}^{\mathrm{T}}\mathbf{b}^*) \right], \end{cases}$$

$$\begin{cases} \mathbf{g}_n^{(2)} = -2\varepsilon_0 (1 + (d_0/c_0)^n)\, \mathrm{Im}[a_n^0]\mathbf{i}_4, \\ \hat{\mathbf{g}}_n^{(2)} = 2\varepsilon_0 (1 - (d_0/c_0)^n)\, \mathrm{Re}[a_n^0]\mathbf{i}_4, \end{cases} \tag{32}$$

in which $\mathbf{g}_n$ and $\hat{\mathbf{g}}_n$ are all divided into two parts: the first part associates to the traction-free condition, and the second part associates to the electric displacement continuous condition.

Finally, by making the superposition of Eqs. (17) and $(21)_3$, and combining with Eqs. (16) and (32), one can obtain the generalized stress function inside piezoelectric medium as

$$\begin{aligned} &\boldsymbol{\phi} = \boldsymbol{\phi}^{\mathrm{I}} + \boldsymbol{\phi}^{\mathrm{II}} = \boldsymbol{\phi}^{(1)} + \boldsymbol{\phi}^{(2)}, \\ &\boldsymbol{\phi}^{(1)} = 2\sum_{n=1}^{\infty} \mathrm{Re}[\mathbf{B}\langle \varsigma_k^{-n} \rangle (\mathbf{A}^{\mathrm{T}}\mathbf{g}_n^{(1)} + \mathbf{B}^{\mathrm{T}}\mathbf{h}_n^{(1)})] + \frac{1}{\pi} \mathrm{Im}\{\mathbf{B}\langle \ln[z_k(\varsigma_k) - z_{k0}(\varsigma_{k0})] \rangle (\mathbf{A}^{\mathrm{T}}\mathbf{f}^* + \mathbf{B}^{\mathrm{T}}\mathbf{b}^*)\}, \\ &\boldsymbol{\varphi}^{(2)} = 2\sum_{n=1}^{\infty} \mathrm{Re}[\mathbf{B}\langle \varsigma_k^{-n} \rangle (\mathbf{A}^{\mathrm{T}}\mathbf{g}_n^{(2)} + \mathbf{B}^{\mathrm{T}}\mathbf{h}_n^{(2)})], \end{aligned} \tag{33}$$

where $\boldsymbol{\phi}^{(1)}$ and $\boldsymbol{\phi}^{(2)}$ represent the function associated with D–P boundary condition (the generalized traction free) and that with the exact electric condition (the electric displacement continuous) caused by the generalized line dislocation and the generalized line force, respectively. Substituting Eqs. (19), (23) and $(32)_4$ into Eq. $(33)_2$ and using the relation

$$\varsigma_k^{-n}\overline{\varsigma}_{j0}^{-n}/n = -\ln(1-\varsigma_k^{-1}\overline{\varsigma}_{j0}^{-1}), \quad \text{if} \quad |\,\varsigma_k^{-1}\overline{\varsigma}_{j0}^{-1}\,| < 1 \tag{34}$$

one obtains

$$\boldsymbol{\phi}^{(1)} = \frac{1}{\pi}\mathrm{Im}[\mathbf{B}\langle \ln(\varsigma_k - \varsigma_{k0})\rangle(\mathbf{A}^{\mathrm{T}}\mathbf{f}^* + \mathbf{B}^{\mathrm{T}}\mathbf{b}^*)] + \frac{1}{\pi}\sum_{j=1}^{4}\mathrm{Im}[\mathbf{B}\langle \ln(\varsigma_k^{-1} - \overline{\varsigma}_{j0})\rangle\mathbf{B}^{-1}\overline{\mathbf{B}}\mathbf{I}_{\mathbf{j}}(\overline{\mathbf{A}}^{\mathrm{T}}\mathbf{f}^* + \overline{\mathbf{B}}^{\mathrm{T}}\mathbf{b}^*)]. \tag{35a}$$

In which

$$\mathbf{I}_1 = \mathrm{diag}[1,0,0,0], \quad \mathbf{I}_2 = \mathrm{diag}[0,1,0,0], \quad \mathbf{I}_3 = \mathrm{diag}[0,0,1,0], \quad \mathbf{I}_4 = \mathrm{diag}[0,0,0,1], \tag{35b}$$

From Eqs. (24) and (29), the electric potential φ_0 on the hole surface can be expressed as

$$\varphi_{0\Gamma} = 2\,\mathrm{Re}[f_0(\sigma)] = 2\,\mathrm{Re}\sum_{n=1}^{\infty} a_n^0[(1+(d_0/c_0)^n)\cos(n\theta) + \mathrm{i}(1-(d_0/c_0)^n)\sin(n\theta)]. \tag{36}$$

Comparing Eq. $(22)_1$ with Eq. (36) and the single-valued condition, one obtains

$$\begin{aligned} &(\mathbf{h}_n)_4 = 2(1+(d_0/c_0)^n)\,\mathrm{Re}[a_n^0],\\ &(\hat{\mathbf{h}}_n)_4 = 2(1-(d_0/c_0)^n)\,\mathrm{Im}[a_n^0]; \quad n \geqslant 1. \end{aligned} \tag{37}$$

Substituting Eqs. (32) and (37) into Eq. (23), the following relations can be obtained

$$\begin{cases} 2[(1+(d_0/c_0)^n) + \varepsilon_0(1-(d_0/c_0)^n)L_{44}^{-1}]\,\mathrm{Re}[a_n^0] + 2\varepsilon_0(1+(d_0/c_0)^n)L_{4i}^{-1}S_{i4}^{\mathrm{T}}\,\mathrm{Im}[a_n^0] = C_{1n},\\ -2\varepsilon_0(1-(d_0/c_0)^n)L_{4i}^{-1}S_{i4}^{\mathrm{T}}\,\mathrm{Re}[a_n^0] + 2[\varepsilon_0(1+(d_0/c_0)^n)L_{44}^{-1} + (1-(d_0/c_0)^n)]\,\mathrm{Im}[a_n^0] = C_{2n}, \end{cases} \tag{38}$$

in which

$$\begin{cases} C_{1n} = \frac{L_{4j}^{-1}}{n\pi}\left\{S_{ji}^{\mathrm{T}}\,\mathrm{Im}\left[\mathbf{B}\left\langle\frac{1+(d_k/c_k)^n}{\varsigma_{k0}^n}\right\rangle\mathbf{A}^{\mathrm{T}}\right] - \mathrm{Re}\left[\mathbf{B}\left\langle\frac{(d_k/c_k)^n-1}{\varsigma_{k0}^n}\right\rangle\mathbf{A}^{\mathrm{T}}\right]\right\}\mathbf{f}^*\\ \qquad + \frac{L_{4j}^{-1}}{n\pi}\left\{S_{ji}^{\mathrm{T}}\,\mathrm{Im}\left[\mathbf{B}\left\langle\frac{1+(d_k/c_k)^n}{\varsigma_{k0}^n}\right\rangle\mathbf{B}^{\mathrm{T}}\right] - \mathrm{Re}\left[\mathbf{B}\left\langle\frac{(d_k/c_k)^n-1}{\varsigma_{k0}^n}\right\rangle\mathbf{B}^{\mathrm{T}}\right]\right\}\mathbf{b}^*,\\ C_{2n} = \frac{L_{4j}^{-1}}{n\pi}\left\{\mathrm{Im}\left[\mathbf{B}\left\langle\frac{1+(d_k/c_k)^n}{\varsigma_{k0}^n}\right\rangle\mathbf{A}^{\mathrm{T}}\right] + S_{ji}^{\mathrm{T}}\,\mathrm{Re}\left[\mathbf{B}\left\langle\frac{(d_k/c_k)^n-1}{\varsigma_{k0}^n}\right\rangle\mathbf{A}^{\mathrm{T}}\right]\right\}\mathbf{f}^*\\ \qquad + \frac{L_{4j}^{-1}}{n\pi}\left\{\mathrm{Im}\left[\mathbf{B}\left\langle\frac{1+(d_k/c_k)^n}{\varsigma_{k0}^n}\right\rangle\mathbf{B}^{\mathrm{T}}\right] + S_{ji}^{\mathrm{T}}\,\mathrm{Re}\left[\mathbf{B}\left\langle\frac{(d_k/c_k)^n-1}{\varsigma_{k0}^n}\right\rangle\mathbf{B}^{\mathrm{T}}\right]\right\}\mathbf{b}^*, \end{cases} \tag{39}$$

where C_{1n}, C_{2n} are reals. Solving Eq. (39), one gets

$$\begin{aligned} &a_n^0 = \alpha_n/\beta_n,\\ &\alpha_n = \frac{1}{2}[\overline{C}_n(d_0/c_0)^n(1-\varepsilon_0L_{44}^{-1} + \mathrm{i}\varepsilon_0L_{4j}^{-1}S_{j4}^{\mathrm{T}}) - C_n(1+\varepsilon_0L_{44}^{-1} + i\varepsilon_0L_{4j}^{-1}S_{j4}^{\mathrm{T}})],\\ &\beta_n = \{(1-(d_0/c_0)^{2n})[1-(\varepsilon_0L_{44}^{-1})^2 - (\varepsilon_0L_{4j}^{-1}S_{j4}^{\mathrm{T}})^2] - 2\varepsilon_0(1+(d_0/c_0)^{2n})L_{44}^{-1}\},\\ &C_n = C_{1n} + \mathrm{i}C_{2n}. \end{aligned} \tag{40}$$

Employing Eq. (32) and Eq. $(33)_3$, the generalized stress function $\boldsymbol{\phi}^{(2)}$ can be expressed as

$$\boldsymbol{\phi}^{(2)} = 2\varepsilon_0\sum_{n=1}^{\infty}\mathrm{Im}[\mathbf{B}\langle\varsigma_k^{-n}\rangle\mathbf{B}^{-1}(\bar{a}_n^0\mathbf{i}_4 - (d_0/c_0)^n a_n^0\mathbf{i}_4)], \tag{41}$$

where a_n^0 is obtained from Eq. (40) and the following relations have been used

$$\mathbf{A}^{\mathrm{T}} + \mathbf{B}^{\mathrm{T}}\mathbf{L}^{-1}\mathbf{S}^{\mathrm{T}} = \mathbf{B}^{-1}/2, \quad \mathbf{B}^{\mathrm{T}}\mathbf{L}^{-1} = \mathrm{i}\mathbf{B}^{-1}/2. \tag{42}$$

Because the air is a special dielectric without mechanical strength, the above solution is much easier than that with a general piezoelectric inclusion. It is also noted that if the elliptic hole is not a slender one, the insulated condition on its boundary is approximately held, that is, $\varepsilon_0 = 0$ inside the elliptic hole. In this case, $\boldsymbol{\phi}^{(2)}$ vanishes and the present solutions coincide with those by Lu and Williams (1998).

4. Piezoelectric plate with a main crack and a generalized line dislocation

In this section, let the elliptic hole degenerate into a crack along the x_1 axis, and a generalized line dislocation $\mathbf{b}^*$ at point $z_0(x_{10}, x_{20})$ is applied only. Then $c_k = d_k = a/2$ and $c_0 = d_0 = a/2$. The additional generalized stress function $\boldsymbol{\phi}^{(2)}$ can be represented as

$$\boldsymbol{\phi}^{(2)} = -4\varepsilon_0 \sum_{n=1}^{\infty} \mathrm{Im}[\mathbf{B}\langle\varsigma_k^{-n}\rangle\mathbf{B}^{-1}(\mathrm{i}\,\mathrm{Im}\,a_n^0\mathbf{i}_4)]. \tag{43}$$

Eq. (40) is simplified to

$$\begin{aligned} &\mathrm{Im}\,C_n = -C_{2n} = -2\frac{L_{4j}^{-1}}{n\pi}\,\mathrm{Im}\left[\mathbf{B}\left\langle\frac{1}{\varsigma_{k0}^n}\right\rangle\mathbf{B}^{\mathrm{T}}\mathbf{b}^*\right], \\ &\beta_n = -4\varepsilon_0 L_{44}^{-1}, \quad \mathrm{Im}\,a_n^0 = C_{2n}/4\varepsilon_0 L_{44}^{-1}. \end{aligned} \tag{44}$$

Substituting Eq. (44) into Eq. (43), the generalized stress function $\boldsymbol{\phi}^{(2)}$ is reduced to

$$\boldsymbol{\phi}^{(2)} = -\frac{1}{L_{44}^{-1}}\sum_{n=1}^{\infty}\mathrm{Re}[\mathbf{B}\langle\varsigma_k^{-n}\rangle\mathbf{B}^{-1}i_4C_{2n}] = -2\sum_{n=1}^{\infty}\mathrm{Re}\left[\mathbf{B}\left\langle\frac{C_{2n}}{2L_{44}^{-1}}\varsigma_k^{-n}\right\rangle\mathbf{B}^{-1}\mathbf{i}_4\right], \tag{45}$$

in which, we have

$$\begin{aligned} -\sum_{n=1}^{\infty}\frac{C_{2n}}{2L_{44}^{-1}}\varsigma_k^{-n} &= -\sum_{n=1}^{\infty}\frac{\varsigma_k^{-n}L_{4j}^{-1}}{n\pi L_{44}^{-1}}\,\mathrm{Im}\left[\mathbf{B}\left\langle\frac{1}{\varsigma_{l0}^n}\right\rangle\mathbf{B}^{\mathrm{T}}\right]\mathbf{b}^* \\ &= -\sum_{n=1}^{\infty}\frac{L_{4j}^{-1}}{nL_{44}^{-1}}\left(\mathbf{B}\left\langle\frac{1}{\varsigma_k^n\varsigma_{l0}^n}\right\rangle\mathbf{q} + \overline{\mathbf{B}}\left\langle\frac{1}{\varsigma_k^n\overline{\varsigma}_{l0}^n}\right\rangle\overline{\mathbf{q}}\right) \\ &= \frac{L_{4j}^{-1}}{L_{44}^{-1}}[B_{jl}\langle\ln(1-\varsigma_k^{-1}\varsigma_0^{-1})\rangle q_l + \overline{B}_{jl}\langle\ln(1-\varsigma_k^{-1}\overline{\varsigma}_{l0}^{-1})\rangle\bar{q}_l]. \end{aligned} \tag{46}$$

Eqs. (45) and (46) show that the generalized stress function $\boldsymbol{\phi}^{(2)}$ is independent of ε_0. It may be seen that Eq. (46) has the same form as that (Eq. (48) in the reference) given in Gao and Fan (1998).

The generalized stress intensity factors $\mathrm{d}\mathbf{K}(a) = \{\mathrm{d}K_{\mathrm{II}}, \mathrm{d}K_{\mathrm{I}}, \mathrm{d}K_{\mathrm{III}}, \mathrm{d}K_{\mathrm{D}}\}$ at the center crack tip $x_1 = a$ is defined as

$$\mathrm{d}\mathbf{K}(a) = \sqrt{2\pi}\lim_{z_k\to a}\sqrt{(z_k - a)}\boldsymbol{\phi}_{,1}|_{x_2=0}. \tag{47}$$

Substituting Eqs. (33), (35) and (43) into Eq. (47), it is found

$$\begin{aligned} \mathrm{d}\mathbf{K}(a) &= \sqrt{\frac{\pi}{a}} \lim_{\varsigma_k \to 1} \frac{\partial \boldsymbol{\phi}}{\partial \varsigma_k} \\ &= \sqrt{\frac{1}{\pi a}} \left\{ \mathrm{Im}\left[\mathbf{B} \left\langle \frac{1}{1-\varsigma_{k0}} \right\rangle \mathbf{B}^{\mathrm{T}} \right] - \sum_{j=1}^{4} \mathrm{Im}\left[\mathbf{B} \left\langle \frac{1}{1-\overline{\varsigma}_{j0}} \right\rangle \mathbf{B}^{-1} \overline{\mathbf{B}} \mathbf{I}_j \overline{\mathbf{B}}^{\mathrm{T}} \right] \right\} \mathbf{b}^* \\ &\quad - \frac{2}{\sqrt{\pi a}} \frac{L_{4j}^{-1}}{L_{44}^{-1}} \mathrm{Im}\left[\mathbf{B} \left\langle \frac{1}{1-\varsigma_{k0}} \right\rangle \mathbf{B}^{\mathrm{T}} \mathbf{b}^* \mathbf{i}_4 \right] \\ &= \sqrt{\frac{1}{\pi a}} \left\{ \mathrm{Im}\left[\mathbf{B} \left\langle 1 - \sqrt{\frac{z_{k0}+a}{z_{k0}-a}} \right\rangle \mathbf{B}^{\mathrm{T}} \mathbf{b}^* \right] - \frac{L_{4j}^{-1}}{L_{44}^{-1}} \mathrm{Im}\left[\mathbf{B} \left\langle 1 - \sqrt{\frac{z_{k0}+a}{z_{k0}-a}} \right\rangle \mathbf{B}^{\mathrm{T}} \mathbf{b}^* \mathbf{i}_4 \right] \right\}. \end{aligned} \tag{48}$$

From Eq. (48), we can obtain

$$\mathrm{d}K_{\mathrm{D}}(a) = -\frac{L_{4j}^{-1}}{L_{44}^{-1}} \mathrm{d}K_j(a), \quad j = 1,2,3. \tag{49}$$

Eq. (49) means that the electric displacement intensity factor caused by generalized line dislocation $\mathbf{b}^*$ in a piezoelectric medium is dependent on the mechanical stress intensity factors and material properties.

Similarly, the generalized stress intensity factors at the center crack tip $x_1 = -a$ are

$$\mathrm{d}\mathbf{K}(-a) = -\sqrt{\frac{1}{\pi a}} \left\{ \mathrm{Im}\left[\mathbf{B} \left\langle 1 - \sqrt{\frac{z_{k0}-a}{z_{k0}+a}} \right\rangle \mathbf{B}^{\mathrm{T}} \mathbf{b}^* \right] - \frac{L_{4j}^{-1}}{L_{44}^{-1}} \mathrm{Im}\left[\mathbf{B} \left\langle 1 - \sqrt{\frac{z_{k0}-a}{z_{k0}+a}} \right\rangle \mathbf{B}^{\mathrm{T}} \mathbf{b}^* \mathbf{i}_4 \right] \right\},$$

$$\mathrm{d}K_{\mathrm{D}}(-a) = -\frac{L_{4j}^{-1}}{L_{44}^{-1}} \mathrm{d}K_j(-a), \quad j = 1,2,3. \tag{50}$$

5. Continuous distribution dislocation method

Here, a small crack is represented by continuous distributed generalized line dislocations. Using the Green's functions obtained in Sections 3 and 4, a group of singular integral equations of the Cauchy type are obtained, which can be solved by a special numerical technique (Erdogan and Gupta, 1972; Hills, 1995).

Let a small crack located near the end of an elliptic hole in plane piezoelectric medium be subjected to uniform electro-mechanical loads at infinity, see Fig. 1. Owing to the linear property, the principle of superposition can be used and the problem can be divided into two ones: (a) The plane piezoelectric medium with an elliptic hole only is subjected to uniform electro-mechanical loads at infinity. (b) Same as the original problem but without electro-mechanical loads at infinity and the small crack is instead by continuous distribution of dislocations. The dislocations will produce tractions on the small crack surface to counteract those produced in problem(a).

For problem (a), the generalized stress function is (Gao and Fan, 1999; Kuang and Ma, 2002)

$$\boldsymbol{\phi}^{(a)} = \boldsymbol{\sigma}_2^{\infty} x_1 - \boldsymbol{\sigma}_1^{\infty} x_2 - \mathrm{Re}\{\mathbf{B} \langle \varsigma_k^{-1} \rangle \mathbf{B}^{-1} [a(\boldsymbol{\sigma}_2^{\infty} - D_2^* \mathbf{i}_4) - \mathrm{i}b(\boldsymbol{\sigma}_1^{\infty} - D_1^* \mathbf{i}_4)]\}, \tag{51}$$

where the uniform loads at infinity can be represented as

$$\boldsymbol{\sigma}_1^{\infty} = [\sigma_{11}^0, \sigma_{12}^0, \sigma_{13}^0, D_1^0]^{\mathrm{T}}, \quad \boldsymbol{\sigma}_2^{\infty} = [\sigma_{21}^0, \sigma_{22}^0, \sigma_{23}^0, D_2^0]^{\mathrm{T}}, \tag{52}$$

and D_1^*, D_2^* are the electric displacement inside the elliptic hole and are given by

$$\begin{cases} (bL_{44}^{-1} - a/\varepsilon_0)D_1^* - aL_{4i}^{-1}S_{i4}^{\mathrm{T}}D_2^* = bL_{4i}^{-1}\sigma_{1i}^{\infty} - aL_{4i}^{-1}S_{ij}^{\mathrm{T}}\sigma_{2i}^{\infty}, \\ bL_{4i}^{-1}S_{i4}^{\mathrm{T}}D_1^* + (aL_{44}^{-1} - b/\varepsilon_0)D_2^* = bL_{4i}^{-1}S_{ij}^{\mathrm{T}}\sigma_{1i}^{\infty} + aL_{4i}^{-1}\sigma_{2i}^{\infty}. \end{cases} \tag{53}$$

If the elliptic hole is degenerated into a center crack along the x_1 axis, let $b = 0$, then Eqs. (51) and (53) are reduced to

$$\begin{aligned} &\boldsymbol{\phi}^{(a)} = \boldsymbol{\sigma}_2^{\infty}x_1 - \boldsymbol{\sigma}_1^{\infty}x_2 - \mathrm{Re}[\mathbf{B}\langle\varsigma_k^{-1}\rangle\mathbf{B}^{-1}a(\boldsymbol{\sigma}_2^{\infty} - D_2^*\mathbf{i}_4)], \\ &D_2^* = L_{4i}^{-1}\sigma_{2i}^{\infty}/L_{44}^{-1} \end{aligned} \tag{54}$$

it can be seen that electric displacement D_2^* only depends on external loads and piezoelectric material properties.

For problem (b), by integrating the generalized stress function, given by Eqs. (35) and (41), along the small crack surface, one obtains

$$\begin{aligned} \phi^{(b)}(\eta) = \frac{1}{\pi}\int_{-c}^{c}\left\{\mathrm{Im}[\mathbf{B}\langle\ln(\varsigma_k - \varsigma_{k0})\rangle\mathbf{B}^{\mathrm{T}}] + \sum_{j=1}^{4}\mathrm{Im}[\mathbf{B}\langle\ln(\varsigma_k^{-1} - \overline{\varsigma}_{j0})\rangle\mathbf{B}^{-1}\overline{\mathbf{B}}\mathbf{I}_j\overline{\mathbf{B}}^{\mathrm{T}}]\right\}\mathbf{b}^*(\xi)\,\mathrm{d}\xi \\ + 2\varepsilon_0\int_{-c}^{c}\sum_{n=1}^{\infty}\mathrm{Im}[\mathbf{B}\langle\varsigma_k^{-n}\rangle\mathbf{B}^{-1}\{\bar{a}_n^0 - (d_0/c_0)^n a_n^0\}]\mathbf{i}_4\,\mathrm{d}\xi, \end{aligned} \tag{55}$$

where $2c$ is the length of the small crack and z_k, z_{k0} can be expressed as

$$\begin{aligned} z_k &= (x_1^0 + p_k x_2^0) + \eta(\cos\alpha + p_k\sin\alpha), \\ z_{k0} &= (x_1^0 + p_k x_2^0) + \xi(\cos\alpha + p_k\sin\alpha), \end{aligned} \tag{56}$$

where α is the angle between the small crack and the axis ox_1, η and ξ denote the distances from the small crack center (x_1^0, x_2^0 or d, ψ) to z_k, z_{k0}, respectively.

Using the superposition principle, the generalized stress function $\boldsymbol{\phi}$ can be expressed as

$$\boldsymbol{\phi} = \boldsymbol{\phi}^{(a)} + \boldsymbol{\phi}^{(b)}. \tag{57}$$

Because the traction is free on the small crack surface, we have

$$\frac{\partial\boldsymbol{\phi}}{\partial s} = \frac{\partial\boldsymbol{\phi}^{(a)}}{\partial s} + \frac{\partial\boldsymbol{\phi}^{(b)}}{\partial s} = 0, \quad |\,s\,| < c. \tag{58}$$

Substituting Eqs. (51) and (55) into Eq. (58), one obtains

$$\begin{aligned} &-\frac{1}{\pi}\int_{-c}^{c}\mathrm{Im}\left[\mathbf{B}\mathbf{B}^{\mathrm{T}}\mathbf{b}^*(\xi)\frac{1}{\xi - \eta}\right]\mathrm{d}\xi + \int_{-c}^{c}\mathbf{K}_1(\xi,\eta)\mathbf{b}^*(\xi)\,\mathrm{d}\xi + \int_{-c}^{c}\mathbf{K}_2(\xi,\eta)\,\mathrm{d}\xi = -\mathbf{T}_{\underline{m}}^{a}(\eta), \\ &\mathbf{T}_{\underline{m}}^{a} = \boldsymbol{\sigma}_2^{\infty}\cos\theta - \boldsymbol{\sigma}_1^{\infty}\sin\theta + \mathrm{Re}\left\{\mathbf{B}\left\langle\frac{\partial\varsigma_k/\partial s}{\varsigma_k^2}\right\rangle\mathbf{B}^{-1}[a(\boldsymbol{\sigma}_2^{\infty} - D_2^*\mathbf{i}_4) - \mathrm{i}b(\boldsymbol{\sigma}_1^{\infty} - D_1^*\mathbf{i}_4)]\right\}, \end{aligned} \tag{59}$$

where $\mathbf{T}_{\underline{m}}^{a}$ denotes the generalized traction along the small crack induced by problem (a) and the kernel functions of the singular integral equation, $\mathbf{K}_1$ and $\mathbf{K}_2$, are

$$\begin{aligned} \mathbf{K}_1(\xi,\eta) &= -\frac{1}{\pi}\mathrm{Im}\left[\mathbf{B}\left\langle\frac{\partial\varsigma_k/\partial s}{\varsigma_k(\varsigma_k\varsigma_{k0} - 1)}\right\rangle\mathbf{B}^{\mathrm{T}}\right] - \frac{1}{\pi}\sum_{l=1}^{4}\mathrm{Im}\left[\mathbf{B}\left\langle\frac{\partial\varsigma_k/\partial s}{\varsigma_k(1 - \varsigma_k\overline{\varsigma}_{l0})}\right\rangle\mathbf{B}^{-1}\overline{\mathbf{B}}\mathbf{I}_l\overline{\mathbf{B}}^{\mathrm{T}}\right], \\ \mathbf{K}_2(\xi,\eta) &= -2\varepsilon_0\sum_{n=1}^{\infty}\mathrm{Im}\left[\mathbf{B}\left\langle\frac{n\partial\varsigma_k/\partial s}{\varsigma_k^{n+1}}\right\rangle\mathbf{B}^{-1}\{\bar{a}_n^0 - (d_0/c_0)^n a_n^0\}\right]\mathbf{i}_4. \end{aligned} \tag{60}$$

It should be noted that in the derivation of Eq. (59), the following relations have been used

$$\begin{aligned}&\frac{\partial}{\partial s}f(z_k)=\frac{\partial f}{\partial x_1}\frac{\partial x_1}{\partial s}+\frac{\partial f}{\partial x_2}\frac{\partial x_2}{\partial s}=\cos\theta\frac{\partial f}{\partial z_k}+p_k\sin\theta\frac{\partial f}{\partial z_k}=(\cos\theta+p_k\sin\theta)\frac{\partial f(z_k)}{\partial z_k},\\&\partial\varsigma_k/\partial s=\frac{2\varsigma_k^2(\cos\theta+p_k\sin\theta)}{a(\varsigma_k^2-1)}.\end{aligned}\tag{61}$$

When the elliptic hole is degenerated into a crack, the Kernel function $\mathbf{K}_2$ can be written as

$$\mathbf{K}_2(\xi,\eta)=\frac{1}{\pi}\mathrm{Im}\left\{\mathbf{B}\left\langle\frac{L_{4j}^{-1}}{L_{44}^{-1}}\left[B_{jl}\left\langle\frac{\partial\varsigma_k/\partial s}{\varsigma_k(\varsigma_k\varsigma_{10}-1)}\right\rangle B_{lm}^{\mathrm{T}}-\overline{B}_{jl}\left\langle\frac{\partial\varsigma_k/\partial s}{\varsigma_k(\varsigma_k\bar{\varsigma}_{l0}-1)}\right\rangle\overline{B}_{lm}^{\mathrm{T}}\right]b_m^*\right\rangle\mathbf{B}^{-1}\right\}\mathbf{i}_4.\tag{62}$$

Let $l'=\xi/c$, $l=\eta/c$, then Eq. (59) can be rewritten as

$$-\frac{1}{\pi}\int_{-1}^{1}\mathrm{Im}[\mathbf{B}\mathbf{B}^{\mathrm{T}}]\mathbf{b}^*(l')\frac{1}{l'-l}\,\mathrm{d}l'+\int_{-1}^{1}\mathbf{K}_1(l',l)\mathbf{b}^*(l')\,\mathrm{d}l'+\int_{-1}^{1}\mathbf{K}_2(l',l)\,\mathrm{d}l'=-\mathbf{T}_{\underline{m}}^a(l),\quad |\,l\,|<1.\tag{63}$$

The single-valued conditions of the generalized displacement around a closed contour surrounding the whole small crack are

$$\int_{-1}^{1}\mathbf{b}^*(l')\,\mathrm{d}l'=\mathbf{0}.\tag{64}$$

Following Erdogan and Gupta (1972), since $\mathbf{b}^*$ have an integrable singularity, we can define a regular unknown function $\widehat{\mathbf{b}}$ as

$$\mathbf{b}^*(l')=\frac{\widehat{\mathbf{b}}(l')}{\sqrt{1-l'^2}},\tag{65}$$

where $\widehat{\mathbf{b}}$ is Holder-continuous along $[-1,1]$.

Now, the whole problem is reduced to a group of singular integral equations including Eqs. (63)–(65). By applying the numerical method introduced by Erdogan and Gupta (1972) and Hills (1995), the unknown function $\widehat{\mathbf{b}}$ can be solved and then the dislocation density $\mathbf{b}^*$ can be determined simply. Here, we select the collocation points l_i', l_r in the interval $[-1,1]$ as

$$l_i'=\cos\frac{(2\mathrm{i}-1)\pi}{2n},\quad l_r=\cos\frac{\pi r}{n},\quad i=1,2,\ldots,n\ \text{ and }\ r=1,2,\ldots,n-1,\tag{66}$$

then the singular integral equations are reduced to a set of algebraic equations as follows

$$\begin{aligned}&\sum_{i=1}^{n}\frac{1}{n}\,\widehat{\mathbf{b}}(l_i')\left\{\frac{\mathrm{Im}[\mathbf{B}\mathbf{B}^{\mathrm{T}}]}{l_i'-l_r}-\pi\mathbf{K}_1(l_i',l_r)-\pi\widehat{\mathbf{K}}_2(l_i',l_r)\right\}=\mathbf{T}_{\underline{m}}^a(l_r),\\&\sum_{i=1}^{n}\widehat{\mathbf{b}}(l_i')=\mathbf{0},\end{aligned}\tag{67a}$$

in which

$$\hat{\mathbf{K}}_2(\xi,\eta)=\frac{1}{\pi}\mathrm{Im}\left\{\mathbf{B}\left\langle\frac{L_{4j}^{-1}}{L_{44}^{-1}}\left[B_{jl}\left\langle\frac{\partial\varsigma_k/\partial s}{\varsigma_k(\varsigma_k\varsigma_{l0}-1)}\right\rangle B_{lm}^{\mathrm{T}}-\overline{B}_{jl}\left\langle\frac{\partial\varsigma_k/\partial s}{\varsigma_k(\varsigma_k\bar{\varsigma}_{l0}-1)}\right\rangle\overline{B}_{lm}^{\mathrm{T}}\right]\right\rangle\mathbf{B}^{-1}\right\}\mathbf{i}_4,\tag{67b}$$

where $\widehat{\mathbf{b}}$ is a four rank vector. The first and second equations of Eq. (67a) will provide $4(n-1)$ and 4 algebraic equations respectively, so Eq. (67a) has totally $4n$ equations with $4n$ unknown variables. The $4n\times4n$ algebraic coefficient matrix on the left hand side of Eq. (67a) can be inversed.

When the function $\widehat{\mathbf{b}}$ is obtained at the collocation points, its value at the two crack tip can be given by (Hills, 1995)

$$\begin{aligned}&\widehat{\mathbf{b}}(1)=M_E(1)\sum_{i=1}^{n}b_E(1)\,\widehat{\mathbf{b}}(l_i'),\quad \widehat{\mathbf{b}}(-1)=M_E(-1)\sum_{i=1}^{n}b_E(-1)\,\widehat{\mathbf{b}}(l_{n+1-i}'),\\&M_E(1)=M_E(-1)=1/n,\quad b_E(1)=b_E(-1)=\frac{\sin[(2i-1)(2n-1)\pi/4n]}{\sin[(2i-1)\pi/4n]}.\end{aligned}\tag{68}$$

The generalized stress vector near the small crack tips can be expressed as

$$\mathbf{T}_{\underline{m}}(l)=\mathrm{i}\mathbf{B}\mathbf{B}^{\mathrm{T}}\frac{\widehat{\mathbf{b}}(l)}{\sqrt{l^2-1}}\mathrm{sgn}(l)+\mathbf{T}^{r}_{\underline{m}}(l),\quad |\,l\,|>1,\tag{69}$$

where $\mathbf{T}^{r}_{\underline{m}}(l)$ is finite near the crack-tips, and sign(l)=l/|l|. When l approaches to 1 (or -1), the values of $\widehat{\mathbf{b}}$ at the tips can be obtained as

$$\widehat{\mathbf{b}}(\pm1)=\lim_{l^{+}\to\pm1}\widehat{\mathbf{b}}(l)=-\lim_{l^{-}\to\pm1}\widehat{\mathbf{b}}(l),\tag{70}$$

where l^{-} means l approaches to ±1 from the outside of the interval $[-1,1]$ and l^{+} means l approaches to ±1 from the inside of the interval $[-1,1]$. Using Eqs. (69) and (70), we can calculate the generalized stress intensity factors at the tips of small crack as follows

$$\begin{Bmatrix}K^{m}_{\mathrm{I}}\\K^{m}_{\mathrm{II}}\\K^{m}_{\mathrm{III}}\\K^{m}_{\mathrm{D}}\end{Bmatrix}=\lim_{x\to\pm c}\sqrt{2\pi(\pm x-c)}\mathbf{F}\mathbf{T}_{\underline{m}}(x)=\lim_{l^{-}\to\pm1}\sqrt{2\pi(\pm l-1)c}\mathbf{F}\mathbf{T}_{\underline{m}}(l)=-\mathrm{i}\sqrt{\pi c}\mathbf{F}\mathbf{B}\mathbf{B}^{\mathrm{T}}\,\widehat{\mathbf{b}}(\pm1)\mathrm{sgn}(\pm1),\tag{71}$$

$\mathbf{F}$ is the transformation matrix given as

$$\mathbf{F}=\begin{bmatrix}-\sin\theta&\cos\theta&0&0\\\cos\theta&\sin\theta&0&0\\0&0&1&0\\0&0&0&1\end{bmatrix}.\tag{72}$$

If the elliptic hole is degenerated into a main crack, the generalized stress intensity factors near the tips of the main crack can be written as two parts, that is

$$\begin{Bmatrix}K_{\mathrm{II}}\\K_{\mathrm{I}}\\K_{\mathrm{III}}\\K_{\mathrm{D}}\end{Bmatrix}=\mathbf{K}^{0}+\overline{\mathbf{K}},\tag{73}$$

where the first part is associated with the uniform loading at infinity, it is

$$\mathbf{K}^{0}=\sqrt{\pi a}(\boldsymbol{\sigma}_2^{\infty}-D_2^{*}\mathbf{i}_4),\tag{74}$$

and the second part, called as the additive generalized stress intensity factors, is produced due to the small crack. Integrating Eq. (48) along the small crack surface, we have

$$\overline{\mathbf{K}}=\int_{-c}^{c}\mathrm{d}\overline{\mathbf{K}}=\int_{-1}^{1}\mathbf{P}(t)\mathbf{b}^{*}(l')\,\mathrm{d}l'=\frac{\pi}{n}\sum_{i=1}^{n}\mathbf{P}(l_i')\,\widehat{\mathbf{b}}(l_i'),\tag{75}$$

where **P** is a bounded complicate function in the interval $[-1,1]$ and is not given here in order to keep this work in a reasonable size.

6. Numerical results and discussions

The numerical examples are carried out for PZT-4 material with the poling direction along the ox_2 axis. The material properties are

$$c_{11} = 13.9 \times 10^{10}\,(\mathrm{N/m^2}), \quad c_{13} = 7.78 \times 10^{10}\,(\mathrm{N/m^2}), \quad c_{12} = 7.43 \times 10^{10}\,(\mathrm{N/m^2}),$$
$$c_{22} = 11.3 \times 10^{10}\,(\mathrm{N/m^2}), \quad c_{44} = 2.56 \times 10^{10}\,(\mathrm{N/m^2}),$$
$$e_{31} = -6.98\,(\mathrm{C/m^2}), \quad e_{22} = 13.84\,(\mathrm{C/m^2}), \quad e_{61} = 13.44\,(\mathrm{C/m^2}),$$
$$\varepsilon_{11} = 6.00 \times 10^{-9}\,(\mathrm{C/Vm}), \quad \varepsilon_{22} = 5.47 \times 10^{-9}\,(\mathrm{C/Vm}).$$

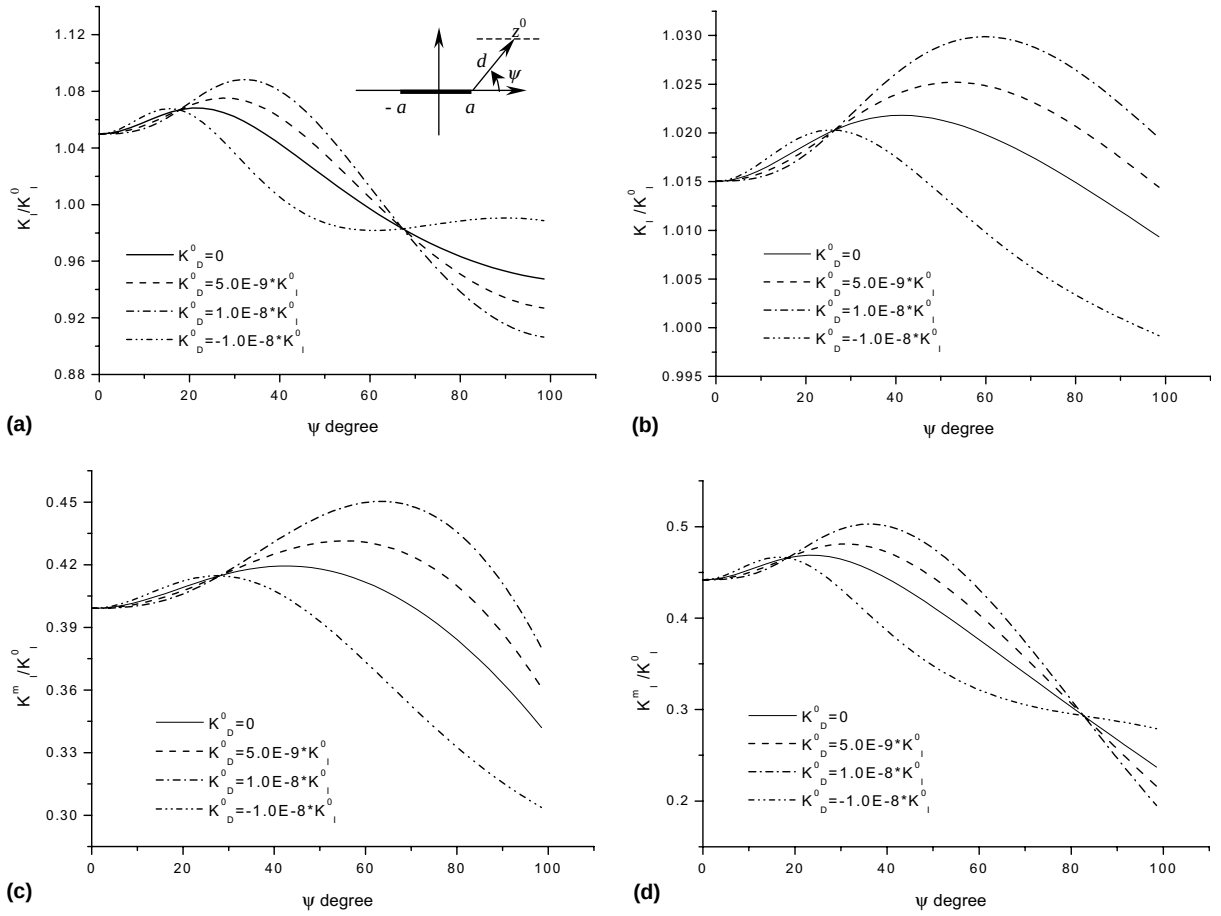

Fig. 2. The distribution of the normalized mechanical intensity factor with ψ for a small crack and a center main crack ($\alpha = 0, d/c = a/c = 2$). (a) At the right tip of main crack. (b) At the left tip of main crack. (c) At the right tip of small crack ($x = c$). (d) At the left tip of small crack ($x = -c$).

Let the center of a small crack be $z^0(x_1^0, x_2^0)$ or (d, ψ) and it inclines an angle α with respect to the axis ox_1, as shown in Fig. 1.

To check the validity of the present method, infinite elastic plate with two same parallel cracks along ox_1 ($d/a = 1.5, a = c, \alpha = \psi = 0$) subjected to Mode I mechanical load σ_2^0 at infinity are considered. The results show that the stress intensity factors at the tips of two cracks are $K_I(a) = 1.22894\sqrt{\pi a}\sigma_2^0$, $K_I(-a) = 1.08107\sqrt{\pi a}\sigma_2^0$ and $K_I(a + d + c) = 1.08108\ \sqrt{\pi a}\sigma_2^0$, $K_I(a + d - c) = 1.22889\sqrt{\pi a}\sigma_2^0$, which are consistent to the results of Han and Chen (1999).

6.1. Interaction between the main crack and a small crack

The second example is to consider the interaction between a small crack and a center main crack with D–P boundary condition and under Mode I electro-mechanical loads at infinity. Both the small crack and the main crack are parallel, that is $\alpha = 0$. For comparing, four kinds of loads ($K_D^0/K_I^0 = 0, 5 \times 10^{-9}$, $10^{-8}, -10^{-8}$) and $d/c = a/c = 2$ are considered.

Fig. 2 shows the variation of the normalized stress intensity factors K_I/K_I^0 and K_I^m/K_I^0 ($K_I^0 = \sqrt{\pi a}\sigma_2^0$) with the angle ψ, respectively. At the right tip of the main crack, the stress intensity factor will be amplified or shielded dependent on the value of ψ. The transition angle from amplifying to shielding depends on the electric load. It is found that in the range of 0–90°, the electric load has no influence on the stress intensity factor at three values ψ. At the left tip of the main crack, the stress intensity factor will always be amplified in the range 0–90° and it is also found that there are two values of ψ at which the electric load has no influence on the stress intensity factor. From Fig. 2, it can also be seen that the normalized stress intensity factors at four tips of small crack and main crack depend on the electric load and the angle ψ. Especially, in some region, negative electric field has a negative influence on the stress intensity factors. The results obtained here are somewhat similar to the results of Fig. 3 in Zeng and Rajapakse's work (2000) for a semi-infinite crack.

Fig. 3 shows the variation of normalized stress intensity factor of main crack with a radial small crack($d/c = 1.2$, $a = 2c$ and $\alpha = \psi$) where the exact electric boundary condition on the boundary of the ellipse is satisfied. As seen from this figure, there are three special ψ values, at which electric field has no influence on the stress intensity factor, including 0° (a parallel small crack) or 90° (a perpendicular small crack) and the third value of ψ (about 38° or 48°) depends on the material properties and the location of the crack. In

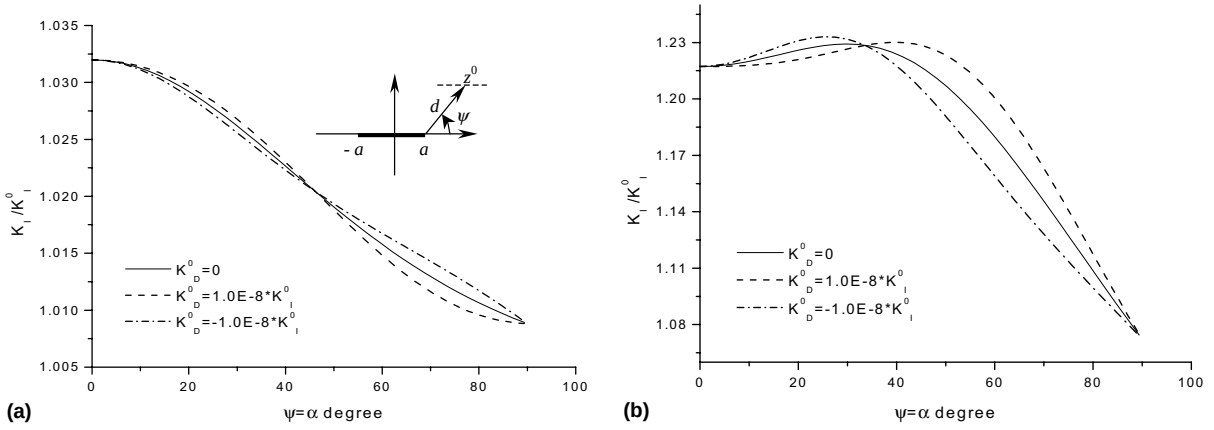

Fig. 3. The distribution of the normalized stress intensity factor near the main crack-tips with ψ for the radial small crack ($\psi = \alpha$, $d/c = 1.2$). (a) At the right main crack-tip. (b) At the left main crack-tip.

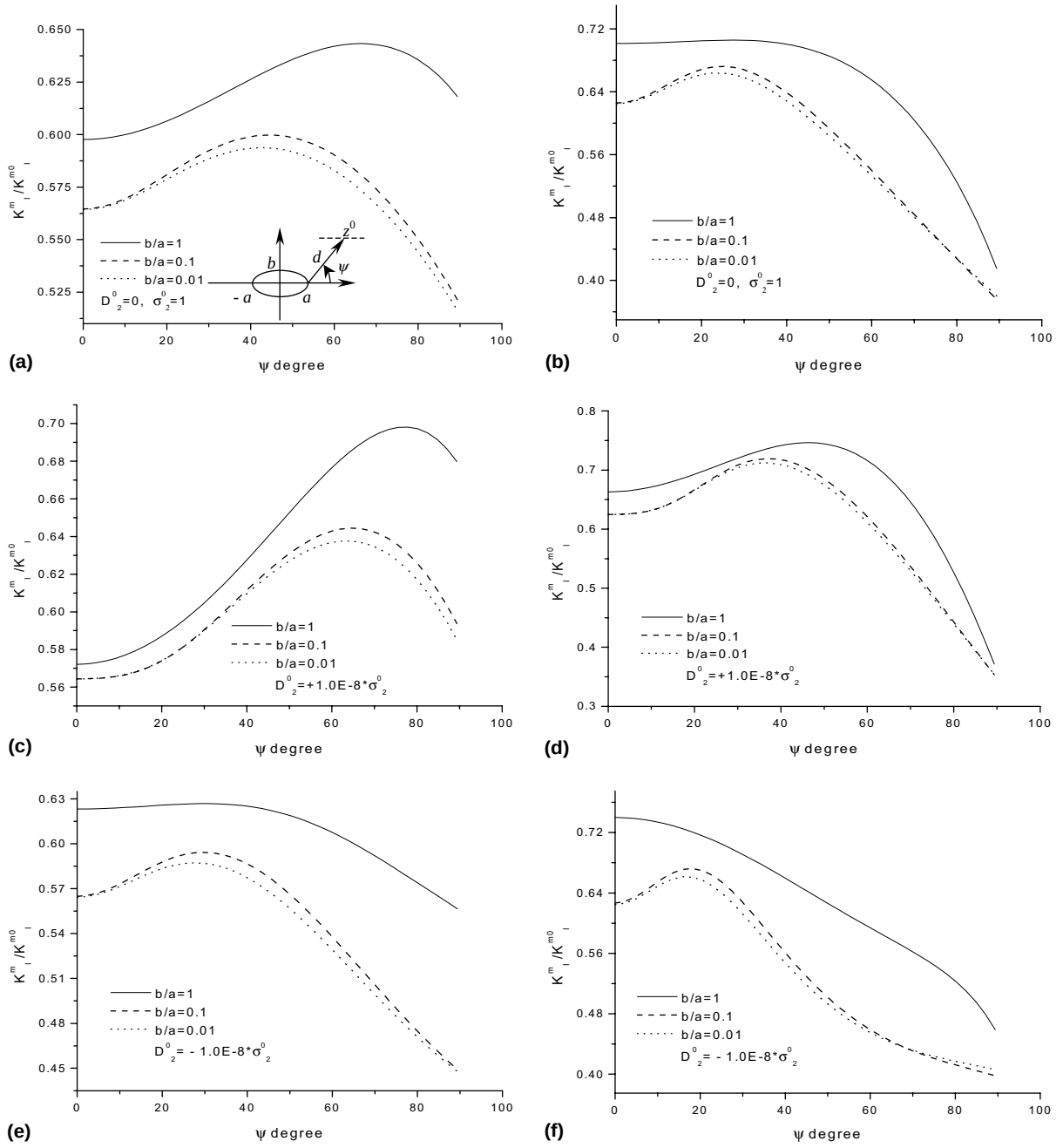

Fig. 4. The distribution of normalized stress intensity factors with ψ ($\alpha = 0, d/c = a/c = 2$). (a) At the right tip of small crack ($x = c$). (b) At the right tip of small crack ($x = c$). (c) At the right tip of small crack ($x = c$). (d) At the left tip of small crack ($x = -c$). (e) At the left tip of small crack ($x = -c$). (f) At the left tip of small crack ($x = -c$).

the region of $\psi \geqslant 0°$, $\alpha \leqslant 90°$, the stress intensity factors at the main crack-tips are always amplified. The negative and positive electric fields will have a contrary effect on the stress intensity factors of the main crack.

6.2. Interactions between the elliptic hole and a small crack

Consider a small crack located near the elliptic hole in a piezoelectric plate subjected to uniform electro-mechanical loads σ_2^0 and D_2^0 at infinity. If the ratio b/a is not very small, the D–P boundary condition is reasonable.

Fig. 4 depicts the distribution of the normalized stress intensity factors $K_{\mathrm{I}}^m/K_{\mathrm{I}}^{m0}$ ($K_{\mathrm{I}}^{m0} = \sqrt{\pi c}\sigma_2^0$) at the end of the small crack with the various angles ψ in a piezoelectric plate subjected to various electro-mechanical loads. As shown in the figure, K_{I}^m of the small crack depends on the ratio b/a, the angle ψ and the electro-mechanical loads. But in all cases, $K_{\mathrm{I}}^m/K_{\mathrm{I}}^{m0} < 1$, which means that an elliptic hole near by the crack can reduce the stress intensity factor of a crack and the shielding effect is happened. It can also be seen that the shielding effect for $D_2 = -1.0 \times 10^{-8}\sigma_2^0$ is larger than that for $D_2 = +1.0 \times 10^{-8}\sigma_2^0$. This means that the direction of the electric field strongly influences the shielding effect. The larger b/a the smaller shielding effect on the stress intensity factors of small crack is, but the effect of b/a on K_{I}^m is very small, when $b/a < 0.01$ and $d = a = 2c$.

Fig. 5 depicts the variation of the normalized stress σ_2/σ_2^0 at the point $(a, 0)$ on the elliptic boundary with the angle ψ. The normalized stress at the right point $(a, 0)$ may be either increased or decreased due to the presence of the small crack. The transition angle is dependent on the electric load and the ratio a/b. Similar to Figs. 2(a) and (b), the electric load has no influence on the stress at three special values of ψ, but in present case the special ψ does not take zero value. As shown in Fig. 5, the positive and negative electric loads have the contrary influence on the stress at the point $(a, 0)$.

Fig. 6 shows the distribution of normalized hoop stress σ_θ/σ_2^0 and electric displacement D_θ/σ_2^0 on the edge of a circle hole ($a = b = 1$) for various radial small crack($\psi = \alpha$, $b/c = a/c = 2$). As shown in Figs. 6(d)–(f), the maximum values of the hoop stress do not always occur at $\theta = 0$ (the polar angle with origin at circle center) and depend on the orientation of radial small crack and electric load. For example, when the mechanical load σ_2^0 is applied only, the maximum values of σ_θ occur at $\theta = 15°$, $\theta = 0°$, $\theta = 23°$ associated with $\psi = 0°$, $\psi = 45°$, $\psi = 90°$, respectively. Similarly, the maximum value of the hoop electric displacement depends on the orientation of radial small crack and electro-mechanical loads.

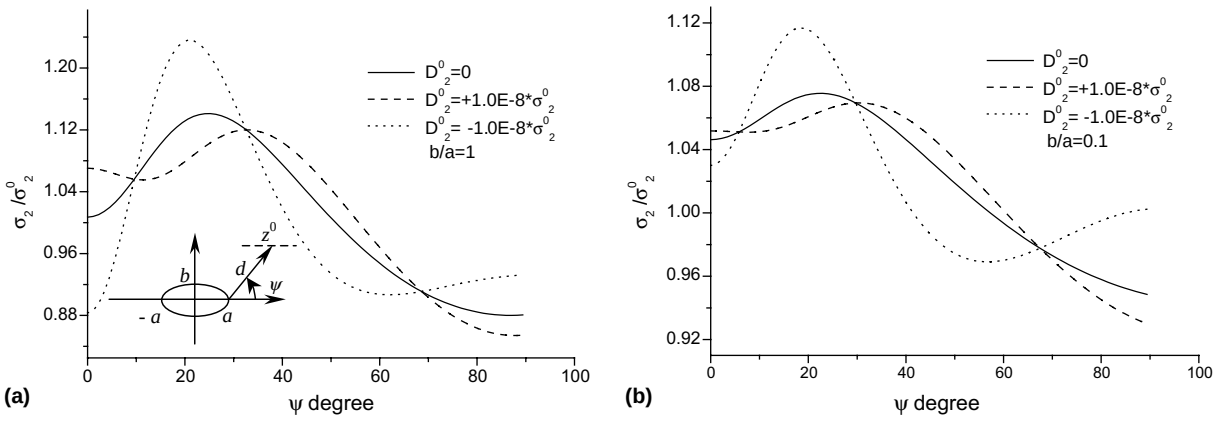

Fig. 5. The normalized stress at the point $(a, 0)$ with ψ the small crack ($\alpha = 0, d/c = a/c = 2$). (a) $b/a = 1$ (b) $b/a = 0.1$.

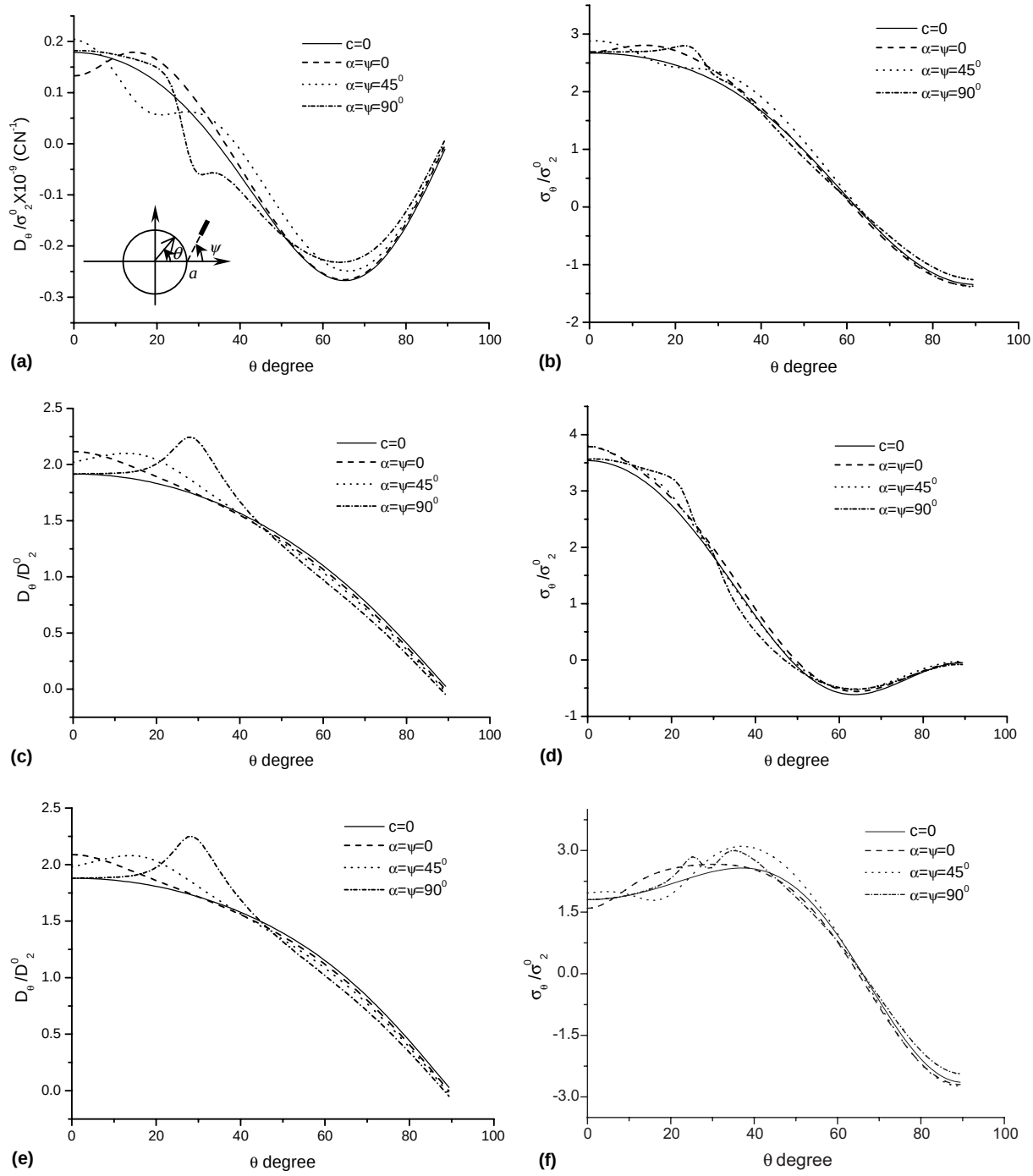

Fig. 6. The distribution of normalized stress and electric displacement on the edge of a circle hole ($\psi = \alpha, d/c = a/c = 2$). (a) $D_2^0 = 0$. (b) $D_2^0 = 1.0\text{E} - 8^*\sigma_2^0$. (c) $D_2^0 = -1.0\text{E} - 8^*\sigma_2^0$. (d) $D_2^0 = 0$. (e) $D_2^0 = 1.0\text{E} - 8^*\sigma_2^0$. (f) $D_2^0 = 1.0\text{E} - 8^*\sigma_2^0$.

7. Conclusions

This paper gives the Green's function for an infinite piezoelectric medium with an elliptic hole filled with air or without air under the generalized line dislocation and the generalized line force. Based on the Green's functions, the interaction of an arbitrary distributed small crack and an elliptic hole in plane piezoelectric medium subjected to uniform electro-mechanical loads at infinity are discussed. Through solving the singular integral equations, the generalized stress intensity factors of main and small cracks with D–P boundary condition or exact electric boundary condition in main crack and the generalized stress on the edge of an elliptic hole are obtained under combined electro-mechanical loads. Numerical illustrations and discussions for the interaction are given. An elliptic hole near by a crack always reduces the stress intensity factors of the crack and the direction of the electric field is important in discussing the shielding effect. The amplifying and shielding to the generalized stress intensity factors of a main crack due to the presence of a small crack are dependent on the location and orientation of a small crack, which is similar with the results in literatures. There are some special locations, at which the electric field has no influence on the stress intensity factor, including 0° (a parallel small crack) and 90° (a perpendicular small crack). The stress and the electric displacement on the edge of an elliptic hole are not always largest at the point $(a, 0)$ when a small crack exists.

Acknowledgment

This work was supported by the National Natural Science Foundation of China through Grants No.10132010 and 10472069.

References

Chung, M.Y., Ting, T.C.T., 1996. Piezoelectric solid with an elliptic inclusion or hole. International Journal of Solids and Structures 33, 3343–3361.

Erdogan, F., Gupta, G.D., 1972. On the numerical solution of singular integral equations. Quarterly of Applied Mathematics 32, 525–534.

Gao, C.F., Fan, W.X., 1998. Green's functions for generalized 2D problems in piezoelectric media with an elliptic hole. Mechanics Research Communications 25 (6), 685–693.

Gao, C.F., Fan, W.X., 1999. Exact solutions for the plane problem in piezoelectric materials with an elliptic or a crack. International Journal of Solids and Structures 36, 2527–2540.

Han, J.J., Chen, Y.H., 1999. Multiple parallel cracks interaction problem in piezoelectric ceramics. International Journal of Solids and Structures 36, 3375–3390.

Hills, D.A., 1995. Solution of Crack Problem. Oxford Press, Oxford.

Huang, Z.Y., Kuang, Z.B., 2001. Dislocation inside a piezoelectric media with an elliptic inhomogeneity. International Journal of Solids and Structures 38, 8459–8479.

Hwu, C., Liang, Y.K., Yen, W.J., 1995. Interactions between inclusions and various types of cracks. International Journal of Fracture 73, 301–323.

Kuang, Z.B., Ma, F.S., 2002. Crack Tip Fields. Xi'an Jiaotong Uinversity Press, Xi'an (in Chinese).

Lu, P., Williams, F.W., 1998. Green functions of piezoelectric material with an elliptic hole or inclusion. International Journal of Solids and Structures 35 (7–8), 651–664.

Pak, Y.E., 1992. Linear electro-elastic fracture mechanics of piezoelectric materials. International Journal of Fracture 54, 79–100.

Park, S.B., Sun, C.T., 1995. Fracture criteria for piezoelectric ceramics. Journal of American Ceramics Society 78, 1475–1480.

Sosa, H., 1991. Plane problems in piezoelectric media with defects. International Journal of Solids and Structures 28, 491–505.

Sosa, H., Khutoryansky, N., 1996. New developments concerning piezoelectric materials with defects. International Journal of Solids and Structures 33 (23), 3399–3414.

Subbarao, E.C., Srikanth, V., Cao, W., Cross, L.E., 1993. Domain switching and small cracking during poling of lead zirconate titanate ceramics. Ferroelectrics 145, 271–281.

Suo, Z., Kuo, C.M., Barnett, D.M., Willis, J.R., 1992. Fracture mechanics for piezoelectric ceramics. Journal of the Mechanics and Physics of Solids 40, 739–765.

Wu, C.C., Freiman, S.W., Rice, R.W., Mecholsky, J.J., 1978. Microstructural aspects of crack propagation in ceramics. Journal of Material Science 13, 2659–2670.

Zeng, X., Rajapakse, R.K.N.D., 2000. Crack amplification and shielding in plane piezoelectric solids. Composites Part B: Engineering 31, 394–404.

Zhou, Z.D., Zhao, S.X., Kuang, Z.B., 2004. Analyses of generalized stress and displacement in piezoelectric ceramics with an elliptic hole. Journal of Shanghai Jiaotong University 38 (8), 1403–1407 (in Chinese).